arXiv:cond-mat/0011206v1 [cond-mat.mtrl-sci] 11 Nov 2000

Quantum kinetic theory of shift current electron pumping in semiconductors

Petr Král[†]

Department of Physics, University of Toronto,
60 St. George Street, Ontario, Toronto M5S 1A7, Canada

[†] *Present address: Department of Chemical Physics,*
Weizmann Institute of Science, 76100 Rehovot, Israel

Abstract

We develop a theory of laser beam generation of *shift currents* in non-centrosymmetric semiconductors. The currents originate when the excited electrons transfer between different bands or scatter inside these bands, and asymmetrically shift their centers of mass in elementary cells. Quantum kinetic equations for hot-carrier distributions and expressions for the induced currents are derived by nonequilibrium Green functions. In applications, we simplify the approach to the Boltzmann limit and use it to model laser-excited GaAs in the presence of LO phonon scattering. The shift currents are calculated in a steady-state regime.

1 Introduction

Photovoltaic phenomena in semiconductors can originate in the built-in or induced asymmetry or inhomogeneity of their crystal structures [1]. In non-centrosymmetric (NCS) crystals, different generation rates for carriers at momenta $\pm\mathbf{k}$ can be induced by asymmetric electron-hole scattering and other processes. The resulting momentum imbalance generates the so called *ballistic current*. Recently [2, 3], this momentum asymmetry of carrier generation in semiconductors was achieved by mixing one- and two-photon transitions at frequencies $2\omega_0$ and ω_0, respectively. In Ref.[4], we describe the effect in GaAs in the presence of scattering on LO phonons. We have also suggested that the current induced by this two-beam coherent control could drive intercalated atoms in carbon nanotubes [5].

In bulk NCS semiconductors, light induced interband transitions of electrons in reciprocal space are accompanied by their *asymmetrical shifts* in the real space between atoms in elementary cells. Similar shifts occur if the transitions are induced by scattering or in recombination. First realistic description of analogous effects in magnetic materials was given by Luttinger [6]. The carrier shifts generate the so called *shift current* [7, 8, 9, 10], which has in general three components, excitation $\mathbf{J_e}$, scattering $\mathbf{J_s}$ and recombination $\mathbf{J_r}$, named after the corresponding processes. The carrier transitions and the related currents are symbolically sketched in Fig.1a. The ballistic current and the excitation part of the shift current $\mathbf{J_e}$ in GaAs were investigated analytically in Ref.[11]; $\mathbf{J_e}$ induced by transitions between light and heavy hole bands was also studied [12]. A summary of older results about the shift current is presented in Ref.[1], but the derivations of the relevant formulas is less clearly documented.

Here, we develop a quantum kinetic theory for the shift current induced by laser excitation and scattering. The expressions for the current components and the transport equations for carrier populations are derived by nonequilibrium Green functions [13] (NGF). In applications, we simplify the approach to the Boltzmann limit and use it to study optically excited GaAs in the presence of scattering by LO phonons. In our modeling, we consider steady-state excitations by a linearly polarized light, and find that $\mathbf{J_e}$ is reasonably large, while $\mathbf{J_s}$ is two orders smaller and $\mathbf{J_r}$ is negligible. Therefore, *continuous electron pumping* through the crystal can be achieved. The ultrafast response of $\mathbf{J_e}$, without additional saturation and relaxation tails from $\mathbf{J_s}$ and $\mathbf{J_r}$, could be useful in opto-electrical applications.

The paper is organized as follows. In Sec.2 we describe our model system. Section 3 is devoted to derivation of expressions for the current components. In Sec.4 these expressions are further approximated. Numerical results for the hot-electron populations and the induced currents in GaAs are presented in Sec.5.

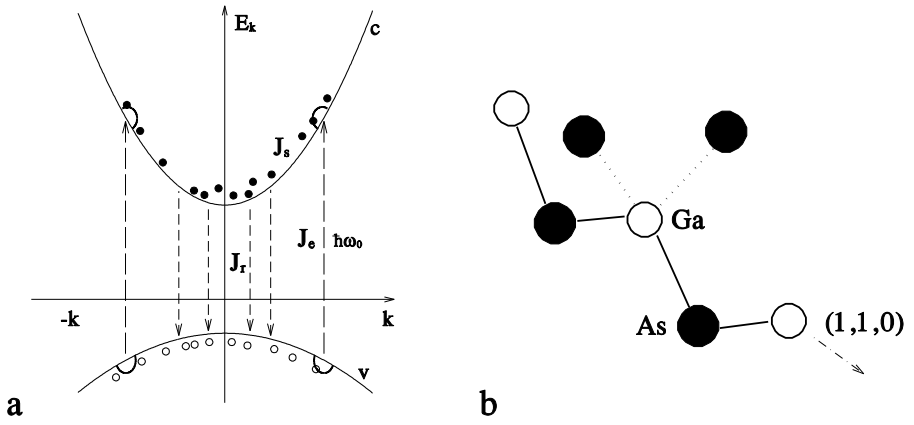

Figure 1: Scheme of the shift current generation in a NCS semiconductor is shown in the inset a). The current has three components, related with the process of electron excitation $\mathbf{J_e}$, scattering $\mathbf{J_s}$ and recombination $\mathbf{J_r}$. They result as a consequence of real space shifts of electrons in the elementary cells that undergo the corresponding transitions in reciprocal space. In the inset b) we show a small section of a zinc-blend structure in GaAs. The excitation conditions and the generated shift currents $\mathbf{J_{e,s,r}}$ are described in the text.

2 The system studied

The physics of the phenomenon can be understood from Fig.1b, where a segment of the zinc-blend structure for GaAs is shown. The valence band states are predominantly localized around the As atoms, while the conduction band states are shifted toward the Ga atoms. Therefore, if the light is polarized along the (1,1,0) direction, the excited electrons transfer from the As atoms at the *bottom* to the Ga atoms in the middle, giving the excitation current $\mathbf{J_e}$ in the (0,0,-1) direction (negative charge). If the light is polarized in the (1,-1,0) direction, electron transitions along bonds orthogonal to the light polarization, *i.e.* from the As atoms at the *top* to the Ga atoms in the middle, generate $\mathbf{J_e}$ in the (0,0,1) direction. During relaxation, the excited electrons (holes) slightly move their centers of charge and stay close to the Ga (As) atoms. Therefore, $\mathbf{J_s}$ is rather small, as we show in our calculations. On the other hand, scattering redistributes the carrier momenta, so that electrons at Ga atoms recombine symmetrically with holes at all neighbor As atoms, which gives negligible $\mathbf{J_r}$.

2.1 The model Hamiltonian

The space shifts of carriers and the related currents can be calculated from a combination of interband and intraband transitions. The length gauge with the elements of the position operator $\mathbf{x}$ evaluated as in Blount's work [14, 15] gives a convenient basis for the description [16]. Therefore, we model the photo-excited bulk GaAs by

the following Hamiltonian [16]

$$\begin{aligned} H &= \sum_{\alpha;\mathbf{k}} \epsilon_\alpha(\mathbf{k})\ a^\dagger_{\alpha,\mathbf{k}}\ a_{\alpha,\mathbf{k}}\ + \sum_{\mathbf{q}}\ \hbar\omega_{\mathbf{q}}\ b^\dagger_{\mathbf{q}}\ b_{\mathbf{q}} \\ &- \ i\ e\ \mathbf{E}(t)\cdot\Big\{\ \frac{1}{2}\ \sum_{\alpha;\mathbf{k}}\ \Big(a^\dagger_{\alpha,\mathbf{k}}\ \frac{\partial a_{\alpha,\mathbf{k}}}{\partial\mathbf{k}} - \frac{\partial a^\dagger_{\alpha,\mathbf{k}}}{\partial\mathbf{k}}\ a_{\alpha,\mathbf{k}}\Big) - i\sum_{\alpha,\beta;\mathbf{k}}\xi_{\alpha\beta}(\mathbf{k})\ a^\dagger_{\alpha,\mathbf{k}}\ a_{\beta,\mathbf{k}}\Big\} \\ &+ \sum_{\alpha,\beta;\mathbf{k},\mathbf{q}} M_{\alpha\beta}(\mathbf{k},\mathbf{k}-\mathbf{q})\ a^\dagger_{\alpha,\mathbf{k}}\ a_{\beta,\mathbf{k}-\mathbf{q}}\ (b_{\mathbf{q}} + b^\dagger_{-\mathbf{q}})\ , \end{aligned} \tag{1}$$

where coupling to LO phonons is added. Here the creation (annihilation) operators $a^\dagger_{\alpha,\mathbf{k}}$ ($a_{\alpha,\mathbf{k}}$) describe electrons with the band index α at wave vector $\mathbf{k}$ in the Brillouin zone. The operator $b^\dagger_{\mathbf{q}}$ ($b_{\mathbf{q}}$) creates (annihilates) phonons with the wave vector $\mathbf{q}$. The electric field is $\mathbf{E}(t) = \mathbf{E}_{+\omega_0}(t)\ e^{-i\omega_0 t} + \mathbf{E}_{-\omega_0}(t)\ e^{+i\omega_0 t}$, where $\mathbf{E}_{+\omega_0}(t) = \mathbf{E}^*_{-\omega_0}(t)$ are complex envelope functions. Spins are included in the current by a factor of 2 (see Eqn.(12)).

2.2 The matrix elements

The matrix elements $\mathbf{x}_{\alpha\beta}(\mathbf{k},\mathbf{k}')$ for the position operator are defined as [14]

$$\mathbf{x}_{\alpha\beta}(\mathbf{k},\mathbf{k}') = i\ \delta_{\alpha\beta}\ \frac{\partial}{\partial\mathbf{k}}\ \delta(\mathbf{k}-\mathbf{k}') + \delta(\mathbf{k}-\mathbf{k}')\,\xi_{\alpha\beta}(\mathbf{k})\ , \tag{2}$$

where the functions

$$\xi_{\alpha\beta}(\mathbf{k}) = \xi^*_{\beta\alpha}(\mathbf{k}) = \int\limits_{\text{U.C.}} d\mathbf{x}\ u^*_{\alpha\mathbf{k}}(\mathbf{x})\ i\ \frac{\partial}{\partial\mathbf{k}}\ u_{\beta\mathbf{k}}(\mathbf{x}) \tag{3}$$

are integrals over the unit cell of the fast components $u_{\alpha\mathbf{k}}(\mathbf{x})$ in the Bloch wave functions $\psi_{\alpha\mathbf{k}}(\mathbf{x}) = e^{i\mathbf{k}\cdot\mathbf{x}}u_{\alpha\mathbf{k}}(\mathbf{x})$. In the following, we use the name $\mathbf{r}_{\alpha\beta}(\mathbf{k}) = \xi_{\alpha\beta}(\mathbf{k})$ for the band off-diagonal elements $\alpha \neq \beta$. They are related to the *interband* velocity elements by

$$\mathbf{v}_{\alpha\beta}(\mathbf{k}) = \langle\alpha,\mathbf{k}|(-i\hbar/m_e)\nabla|\beta,\mathbf{k}\rangle = \frac{\epsilon_\beta(\mathbf{k}) - \epsilon_\alpha(\mathbf{k})}{i\hbar}\ \mathbf{r}_{\alpha\beta}(\mathbf{k})\ . \tag{4}$$

The electron-phonon matrix elements [17, 18]

$$\begin{aligned} M_{\alpha\beta}(\mathbf{k},\mathbf{k}-\mathbf{q}) &= M(\mathbf{q})\ \gamma_{\alpha\beta}(\mathbf{k},\mathbf{k}-\mathbf{q})\ , \\ \gamma_{\alpha\beta}(\mathbf{k},\mathbf{k}-\mathbf{q}) &= \int\limits_{\text{U.C.}} d\mathbf{x}\ u^*_{\alpha\mathbf{k}}(\mathbf{x})\ u_{\beta\mathbf{k}-\mathbf{q}}(\mathbf{x}) \end{aligned} \tag{5}$$

include the structure factors $\gamma_{\alpha\beta}(\mathbf{k},\mathbf{k}-\mathbf{q})$, which separately depend on the "incoming" and "outgoing" momenta $\gamma_{\alpha\beta}(\mathbf{k},\mathbf{k}-\mathbf{q}) \neq f(\mathbf{q})$. Therefore, the factor $M(\mathbf{q})$ in the expression (5) gives the rate of electron scattering, while the real space shifts of electrons are solely controlled by the lattice [9, 10], determining the factors

$\gamma_{\alpha\beta}(\mathbf{k}, \mathbf{k}-\mathbf{q})$ (see Appendix B). In the approximation of a constant LO phonon energy $\hbar\omega_q \approx \hbar\omega_Q$, the element $M^2(\mathbf{q})$ is given by [18]

$$M^2(\mathbf{q}) = \frac{M_0^2}{|\mathbf{q}|^2} \ , \quad M_0^2 = 2\pi e^2 \hbar\omega_Q \left(\frac{1}{\epsilon_\infty} - \frac{1}{\epsilon_0}\right) \ . \tag{6}$$

The parameters relevant for GaAs are used; $\hbar\omega_Q = 36$ meV, $\epsilon_0 = 12.5$ and $\epsilon_\infty = 10.9$.

3 Description of the system

We describe the problem by nonequilibrium Green functions [19, 20] in the matrix form $G_{\alpha\beta}$, similarly as in Ref.[4]. The shift current can be expressed through the *interband* elements for NGF, which must be known on a semi-analytical level, so that the space shifts can be obtained first by algebraic operations. In older works, the manipulations have been carried out in the density matrix formalism, but the intermediate steps were less clearly presented. More recently, NGF were used to investigate the shift current from electron hopping in superlattices [21], and in other photovoltaic phenomena [22, 23].

Here, we develop an approach similar to Ref.[21], and apply it to our system in a steady-state regime. The interband functions $G_{\alpha\beta}$ ($\alpha \neq \beta$) are expressed from the *differential* version of the Kadanoff-Baym equations [19] (KBE) in terms of the intraband $G_{\alpha\alpha}$ from the scattering integrals of these KBE. Then $G_{\alpha\beta}$ are substituted in the formula for the shift current, where the mentioned reordering is performed. Finally, $G_{\alpha\alpha}$ are calculated numerically from the *integral* version of KBE [4]. We have not been able to perform this reordering, at least for $\mathbf{J}_s$, when $G_{\alpha\beta}$ was expressed from the integral KBE.

3.1 The differential KBE

The differential version of KBE for the matrix correlation function $\mathbf{G}^<$ is [19, 20] ($\chi = (\mathbf{k}, t)$, integration over $\bar{\chi}$ is implied)

$$\left(\mathbf{G}^{R,0}(\chi, \bar{\chi})\right)^{-1} \mathbf{G}^<(\bar{\chi}, \chi') = \left(\mathbf{\Sigma}(\chi, \bar{\chi})\ \mathbf{G}(\bar{\chi}, \chi')\right)^< \ , \tag{7}$$

where $(\mathbf{G}^{R,0})^{-1}{=}(G^{R,0}_{\alpha\beta}\ )^{-1}\delta_{\alpha\beta}$ is the inverted free propagator [19]. The lesser operation $<$ can be applied to the functions on the r.h.s of (7) with the help of the Langreth-Wilkins (LW) rules [24] $(AB)^< = A^< B^A + A^R B^<$. The KBE can be also written in a form, where $(\mathbf{G}^{A,0})^{-1}$ acts on $\mathbf{G}^<$ from the right side, and, in the scattering term, $\mathbf{\Sigma}$ is interchanged with $\mathbf{G}$.

Subtraction of these two KBE gives [20] ($T = (t + t')/2$)

$$i\hbar\ \frac{\partial G^<_{\alpha\beta}(\chi, \chi')}{\partial T} - (\epsilon_\alpha(\mathbf{k}) - \epsilon_\beta(\mathbf{k}'))\ G^<_{\alpha\beta}(\chi, \chi')$$

$$
\begin{aligned}
&= \Sigma_{f;\alpha\bar{\gamma}}(\chi,\bar{\chi})\; G^{<}_{\bar{\gamma}\beta}(\bar{\chi},\chi^{'}) - G^{<}_{\alpha\bar{\gamma}}(\chi,\bar{\chi})\; \Sigma_{f;\bar{\gamma}\beta}(\bar{\chi},\chi^{'}) \\
&+ \left(\Sigma_{s;\alpha\bar{\gamma}}(\chi,\bar{\chi})\; G_{\bar{\gamma}\beta}(\bar{\chi},\chi^{'})\right)^{<} - \left(G_{\alpha\bar{\gamma}}(\chi,\bar{\chi})\; \Sigma_{s;\bar{\gamma}\beta}(\bar{\chi},\chi^{'})\right)^{<} . \qquad (8)
\end{aligned}
$$

In the scattering integrals on the r.h.s., field $\Sigma_{f;\alpha\beta}$ and scattering $\Sigma_{s;\alpha\beta}$ self-energy functions are introduced [4]. The terms do *not* commute because of the time, momentum and band indices. The momentum and band non-commutativity ultimately leads to the shift currents. The time issue should be less serious, if pulse fields with slow envelope functions are applied to the system, where gradient expansions in terms of the difference time τ could be performed around the CMS time coordinate T [19, 25]. We adopt this approach here and include only the zero order terms.

3.2 The self-energy functions

In order to obtain the field self-energy $\Sigma_{f;\alpha\beta}$ for the Hamiltonian (1) in the length gauge, it is necessary to perturbatively expand the Green functions in terms of the light excitation, similarly as in Ref.[4]. Direct calculation gives

$$
\begin{aligned}
\Sigma_{f;\alpha\beta}(\mathbf{k},\mathbf{k}^{'},t,t^{'}) &= -i\; e\; \delta(t-t^{'})\; \delta(\mathbf{k}-\mathbf{k}^{'}) \\
&\times \mathbf{E}(t)\cdot\left\{\frac{1}{2}\left(\frac{\partial}{\partial\mathbf{k}^{'}} - \frac{\partial}{\partial\mathbf{k}}\right)\delta_{\alpha\beta} - i\;\xi_{\alpha\beta}(\mathbf{k})\right\} , \qquad (9)
\end{aligned}
$$

which has zero correlation parts $\Sigma^{<,>}_{f;\alpha\beta}(\mathbf{k},\mathbf{k}^{'},t,t^{'}) = 0$. This self-energy acts as an operator, due to the presence of derivatives. When surrounded by functions with two momenta variables, it differentiates the front (back) function over $\mathbf{k}$ ($\mathbf{k}^{'}$), and set $\mathbf{k} = \mathbf{k}^{'}$. The derivatives can be shifted from one side to the other side by a partial integration, which changes their signs and combines the two with a prefactor 1. We can also introduce its steady-state form

$$
\Sigma^{\pm}_{f;\alpha\beta}(\mathbf{k},\mathbf{k}^{'}) = -i\; e\; \delta(\mathbf{k}-\mathbf{k}^{'})\; \mathbf{E}_{\pm\omega_0}\cdot\left\{\frac{1}{2}\left(\frac{\partial}{\partial\mathbf{k}^{'}} - \frac{\partial}{\partial\mathbf{k}}\right)\delta_{\alpha\beta} - i\;\xi_{\alpha\beta}(\mathbf{k})\right\} , \quad (10)
$$

which can be obtained by a Fourier transform of the Dyson equation in the frequency domain [19]. The frequency argument of the Green functions following $\Sigma^{\pm}_{f;\alpha\beta}$ are shifted by $\mp\omega_0$ (see Ref.[4]).

Finally, we have to write down the correlation function for the electron-phonon self-energy, which we use in the self-consistent Born approximation

$$
\begin{aligned}
\Sigma^{<}_{s;\alpha\beta}(\mathbf{k},\mathbf{k}^{'},t,t^{'}) &= M_{\alpha\gamma}(\mathbf{k},\mathbf{k}-\bar{\mathbf{q}})\; M_{\delta\beta}(\mathbf{k}^{'}-\bar{\mathbf{q}},\mathbf{k}^{'}) \\
&\times G^{<}_{\gamma\delta}(\mathbf{k}-\bar{\mathbf{q}},\mathbf{k}^{'}-\bar{\mathbf{q}},t,t^{'})\; D^{<}(\bar{\mathbf{q}},t,t^{'}) . \qquad (11)
\end{aligned}
$$

Here, the non-locality in momentum and time as well as all kinds of interband transitions are included (summation over $\bar{\mathbf{q}}$ and repeated band indices).

3.3 The total shift current density J

The shift current density $\mathbf{J}$ can be expressed in terms of the *interband* velocity elements $\mathbf{v}_{\beta\alpha}(\mathbf{k})$ and the $\mathbf{k}$-diagonal elements of the correlation functions $G^<_{\alpha\beta}(\mathbf{k},\mathbf{k})$. If the perturbing electric field is homogeneous in real space, *i.e.* invariant with respect to the lattice translation of the crystal, then we would naturally expect that these functions are $\mathbf{k}$-diagonal $G^<_{\alpha\beta}(\mathbf{k},\mathbf{k}') = G^<_{\alpha\beta}(\mathbf{k})\ \delta(\mathbf{k}-\mathbf{k}')\ (2\pi)^3$. In reality, Eqn.(8) for the Hamiltonian (1) in the length gauge should be further transformed [20], to explicitly give zero off-diagonal elements, and this could generate additional terms. In our problem these transforms would be complex, so that we make the *Ansatz* that Eqn.(8) gives momentum diagonal $G^<_{\alpha\beta}$.

The steady-state shift current density $\mathbf{J}$ can be expressed as follows

$$\mathbf{J} = 2e \int \frac{d\hbar\omega}{2\pi} \int \frac{d\mathbf{k}}{(2\pi)^3} \sum_{\alpha\neq\beta} \mathbf{v}_{\beta\alpha}(\mathbf{k})\ G^<_{\alpha\beta}(\mathbf{k},\omega) = \mathbf{J_e} + \mathbf{J_s} + \mathbf{J_r}\ , \tag{12}$$

where the prefactor 2 encounters the spins. The components $\mathbf{J_{e,s,r}}$, which represent contributions of the three processes depicted in Fig.1a, can be obtained, if $\mathbf{v}_{\beta\alpha}$ from (4) and the solution $G^<_{\alpha\beta}$ of Eqn.(8) are substituted in the expression (12). In the steady state, the first term on the l.h.s. of Eqn.(8) is absent. The remaining $G^<_{\alpha\beta}$, expressed through the scaterring integrals on the r.h.s., can be substituted in (12), which was also used in Ref.[21]. In transient situations, the time derivative of $G^<_{\alpha\beta}$ in Eqn.(8) must be also included, but we are postponing this problem to future studies. Terms with equal band indices $\alpha = \beta$ in (12) would give the ballistic current density, calculated in Ref.[4] for excitation by two laser beams.

3.4 The excitation current density $\mathbf{J_e}$

Let us first find the expression for $\mathbf{J_e}$ from the two terms with $\Sigma_{f;\alpha\beta}$ on the r.h.s. of Eqn.(8). Since $\mathbf{J_e}$ results in the second order of the laser field, $\Sigma_{f;\alpha\beta}$ in those terms must be combined with the first order interband correlation functions $G^<_{1;\alpha\beta} \approx \Big(G_{0;\alpha\alpha}\ \Sigma_{f;\alpha\beta}\ G_{0;\beta\beta}\Big)^<$, expressed through the interacting Green functions in the absence of laser field [4] $G_{0;\alpha\alpha}$. The resulting $\mathbf{J_e}$ has the form

$$\begin{aligned}
\mathbf{J_e} \;=\; & 2ie \int \frac{d\omega}{2\pi} \int \frac{d\mathbf{k}}{(2\pi)^3} \sum_{\alpha\neq\beta;\ \gamma} \mathbf{r}_{\beta\alpha}(\mathbf{k}) \\
\times\; & \Big(\Sigma^{\pm}_{f;\alpha\gamma}(\mathbf{k},\bar{\mathbf{k}}_1)\ \Big(G_{0;\gamma\gamma}(\bar{\mathbf{k}}_1,\bar{\mathbf{k}}_2,\omega)\ \Sigma^{\mp}_{f;\gamma\beta}(\bar{\mathbf{k}}_2,\bar{\mathbf{k}}_3)\ G_{0;\beta\beta}(\bar{\mathbf{k}}_3,\mathbf{k},\omega\pm\omega_0)\Big)^< \\
-\; & \Big(G_{0;\alpha\alpha}(\mathbf{k},\bar{\mathbf{k}}_1,\omega)\ \Sigma^{\mp}_{f;\alpha\gamma}(\bar{\mathbf{k}}_1,\bar{\mathbf{k}}_2)\ G_{0;\gamma\gamma}(\bar{\mathbf{k}}_2,\bar{\mathbf{k}}_3,\omega\pm\omega_0)\Big)^<\ \Sigma^{\pm}_{f;\gamma\beta}(\bar{\mathbf{k}}_3,\mathbf{k})\Big)\ ,
\end{aligned} \tag{13}$$

where we neglect vertex corrections to $G^<_{1;\alpha\beta}$, which can contribute especially in transient situations [4], and assume that $G_{0;\alpha\beta} \approx 0$. We also write two momenta

in the equilibrium Green functions $G_{0;\alpha\alpha}(\mathbf{k},\mathbf{k}')$, in order to perform the derivatives from the field self-energies $\Sigma_{f;\alpha\beta}(\mathbf{k},\mathbf{k}')$, even though they fulfill $G_{0;\alpha\alpha}(\mathbf{k},\mathbf{k}') = G_{0;\alpha\alpha}(\mathbf{k})\ \delta(\mathbf{k}-\mathbf{k}')\ (2\pi)^3$ without the above Ansatz. In Appendix A, we show [16] that after algebraic manipulations only elements with $\gamma=\beta$ ($\gamma=\alpha$) remain in the first (second) expression of Eqn.(13).

In total, we obtain the c-component of the vector for the current density $\mathbf{J_e}$

$$\begin{aligned} J_e^c &= 2\ e^3 \int \frac{d\omega}{2\pi} \int \frac{d\mathbf{k}}{(2\pi)^3} \sum_{\alpha\neq\beta} r^a_{\beta\alpha;c}(\mathbf{k})\ r^b_{\alpha\beta}(\mathbf{k})\ E^a_{\pm\omega_0}\ E^b_{\mp\omega_0} \\ &\times \Big(G_{0;\alpha\alpha}(\mathbf{k},\omega)\ G_{0;\beta\beta}(\mathbf{k},\omega\pm\omega_0)\Big)^<\ , \end{aligned} \tag{14}$$

where sum over a and b components is performed. The sign convention and the terms $r^a_{\beta\alpha;c}(\mathbf{k})$ are described in Appendix A. For weak scattering, the expression (14) agrees with density matrix calculations [16]. In this formalism also a nonzero virtual term *below* the band gap can be traced in an expression analogous to (14). It can be canceled by a similar term, with opposite sign, resulting from the band diagonal contribution $\mathbf{v}_{\alpha\alpha}\ G^<_{\alpha\alpha}$ to the current.

For a light linearly polarized in the b-direction, the product of the components $E^b_{\pm\omega_0}$ with $r^b_{\beta\alpha;c}(\mathbf{k})\ r^b_{\alpha\beta}(\mathbf{k})$ can be further simplified. If the matrix elements are used in the form [9, 10] $r^b_{\beta\alpha}(\mathbf{k}) = |r^b_{\beta\alpha}(\mathbf{k})|\ e^{i\phi^b_{\beta\alpha}(\mathbf{k})}$, we can arrange $\mathbf{J}_e$ as follows

$$\begin{aligned} \mathbf{J}_e &= 2\ e^3 \int \frac{d\omega}{2\pi} \int \frac{d\mathbf{k}}{(2\pi)^3} \sum_{\alpha\neq\beta} |E^b_{+\omega_0}|^2 \left(i\ \mathbf{R}^b_{e;\beta\alpha}(\mathbf{k})\ |r^b_{\alpha\beta}(\mathbf{k})|^2 + \frac{1}{2}\frac{\partial\ |r^b_{\alpha\beta}(\mathbf{k})|^2}{\partial\mathbf{k}}\right) \\ &\times \Big(G_{0;\alpha\alpha}(\mathbf{k},\omega)\ G_{0;\beta\beta}(\mathbf{k},\omega\pm\omega_0)\Big)^<\ , \end{aligned} \tag{15}$$

where we have introduced the excitation shift vector $\mathbf{R}^b_{e;\beta\alpha}$ with the c-component

$$R^{b;c}_{e;\beta\alpha}(\mathbf{k}) = \frac{\partial\phi^b_{\beta\alpha}(\mathbf{k})}{\partial k^c} + \xi^c_{\alpha\alpha}(\mathbf{k}) - \xi^c_{\beta\beta}(\mathbf{k})\ . \tag{16}$$

From the expression (16), it follows that the vector is invariant under the phase transformation [9, 10, 16] $\psi_{\beta\mathbf{k}}(\mathbf{x}) \to e^{i\theta_n(\mathbf{k})}\psi_{\beta\mathbf{k}}(\mathbf{x})$ of the Bloch functions $\psi_{\beta\mathbf{k}}(\mathbf{x})$, where $\theta_n(\mathbf{k})$ are arbitrary well-behaved functions. It is also anti-symmetric $\mathbf{R}^b_{e;\beta\alpha}(\mathbf{k}) = -\mathbf{R}^b_{e;\alpha\beta}(\mathbf{k})$ in the band index $\alpha\leftrightarrow\beta$, since $\mathbf{r}_{\alpha\beta}(\mathbf{k}) = (\mathbf{r}_{\beta\alpha}(\mathbf{k}))^*$. Note in (15), that the anti-symmetric $\mathbf{R}^b_{e;\alpha\beta}(\mathbf{k})$ combines with the imaginary (spectral) values from the Green function product, while the band symmetric derivative $\partial|r^b_{\alpha\beta}(\mathbf{k})|^2/\partial\mathbf{k}$ combines with its real (main) part, representing renormalization effects due to interactions. An analogous situation occurs in the scattering shift vector $\mathbf{R}_{s;\beta\beta}(\mathbf{k},\mathbf{k}')$ (see Appendix B) and in the scattering current density $\mathbf{J}_s$, discussed below.

3.5 The scattering current density $\mathbf{J_s}$

The formula for $\mathbf{J_s}$ can be obtained, if the rest two terms from the r.h.s. of Eqn.(8), with the electron-phonon self-energy in (11), are substituted in the expression (12).

In this work, we consider only *intraband* relaxation, so that band-diagonal Green functions are used in $\mathbf{J_s}$. We also assume that they depend on one $\mathbf{k}$ variable, in accordance with our Ansatz.

Let us concentrate first on the two terms $\mathbf{r}$ $(\Sigma^R G^< - G^R \Sigma^<)$, in the expression resulting from (12). They can be written as follows

$$\begin{aligned}
&\sum_{\alpha\neq\beta} \mathbf{r}_{\beta\alpha}(\mathbf{k}) \left(\Sigma^R_{\alpha\beta}(\mathbf{k},\omega)\ G^<_{\beta\beta}(\mathbf{k},\omega) - G^R_{\alpha\alpha}(\mathbf{k},\omega)\ \Sigma^<_{\alpha\beta}(\mathbf{k},\omega) \right) \\
&= \sum_{\alpha\neq\beta;\ \gamma} \mathbf{r}_{\beta\alpha}(\mathbf{k}) M_{\alpha\gamma}(\mathbf{k},\mathbf{k}-\bar{\mathbf{q}}) G^R_{\gamma\gamma}(\mathbf{k}-\bar{\mathbf{q}},\omega-\bar{\omega}) D^>(\bar{\mathbf{q}},\omega-\bar{\omega}) M_{\gamma\beta}(\mathbf{k}-\bar{\mathbf{q}},\mathbf{k}) G^<_{\beta\beta}(\mathbf{k},\omega) \\
&- \sum_{\alpha\neq\beta;\ \gamma} \mathbf{r}_{\beta\alpha}(\mathbf{k}) M_{\alpha\gamma}(\mathbf{k},\mathbf{k}-\bar{\mathbf{q}}) G^<_{\gamma\gamma}(\mathbf{k}-\bar{\mathbf{q}},\omega-\bar{\omega}) D^R(\bar{\mathbf{q}},\omega-\bar{\omega}) M_{\gamma\beta}(\mathbf{k}-\bar{\mathbf{q}},\mathbf{k}) G^<_{\beta\beta}(\mathbf{k},\omega) \\
&- \sum_{\gamma\neq\alpha;\ \beta} \mathbf{r}_{\alpha\gamma}(\mathbf{k}) G^R_{\gamma\gamma}(\mathbf{k},\omega) M_{\gamma\beta}(\mathbf{k},\mathbf{k}-\bar{\mathbf{q}}) G^<_{\beta\beta}(\mathbf{k}-\bar{\mathbf{q}},\omega-\bar{\omega}) D^<(\bar{\mathbf{q}},\omega-\bar{\omega}) M_{\beta\alpha}(\mathbf{k}-\bar{\mathbf{q}},\mathbf{k}) \ ,
\end{aligned} \tag{17}$$

where the band arguments have been shifted in the last term. In the propagator part of the electron-phonon self-energy, the formula $\Sigma^R \propto (GD)^R = G^R D^> - G^< D^R$ has been used, which is valid for functions with this argument ordering [24, 25]. The first term on the r.h.s. of (17), resulting from $G^R\ D^<$, looks similar to the last term, but the two differ in the type of phonon correlation functions $D^>$, $D^<$ and the energy-momentum arguments in $G^<_{\beta\beta}$, $G^R_{\gamma\gamma}$ and $M_{\gamma\beta}$.

This can changed, if the substitution $\mathbf{k}^{'} = \mathbf{k} - \bar{\mathbf{q}}$ and $\omega^{'} = \omega - \bar{\omega}$, followed by $\omega^{''} = -\bar{\omega}$, is used in the last term of (17); we take advantage of the fact that the Bose-Einstein distribution satisfies $n_{BE}(\omega) = 1/(\exp(\hbar\omega/kT) - 1) = -(1 + n_{BE}(-\omega))$. The sum of the first and last terms is

$$\begin{aligned}
&\Big(\sum_{\alpha\neq\beta;\ \gamma} \mathbf{r}_{\beta\alpha}(\mathbf{k})\ M_{\alpha\gamma}(\mathbf{k},\mathbf{k}-\bar{\mathbf{q}}) - \sum_{\gamma\neq\alpha;\ \beta} M_{\beta\alpha}(\mathbf{k},\mathbf{k}-\bar{\mathbf{q}})\ \mathbf{r}_{\alpha\gamma}(\mathbf{k}-\bar{\mathbf{q}}) \Big)\ M_{\gamma\beta}(\mathbf{k}-\bar{\mathbf{q}},\mathbf{k}) \\
&\qquad \times G^R_{\gamma\gamma}(\mathbf{k}-\bar{\mathbf{q}},\omega-\bar{\omega})\ D^>(\bar{\mathbf{q}},\omega-\bar{\omega})\ G^<_{\beta\beta}(\mathbf{k},\omega) \ .
\end{aligned} \tag{18}$$

Here the band indices at the electron propagator and correlation function can be set equal $\gamma = \beta$, because intraband relaxation is considered. The commutator in the large bracket, multiplied by the element $M_{\gamma\beta}(\mathbf{k}-\bar{\mathbf{q}},\mathbf{k})$, can be rewritten in terms of the scattering shift vector $\mathbf{R}_{s;\beta\beta}(\mathbf{k},\mathbf{k}-\bar{\mathbf{q}})$ and a renormalization correction, as shown in Eqn.(B.3). If *interband* relaxation is also considered, the resulting formulas can be generalized analogously.

The other two terms $\mathbf{r}$ $(\Sigma^< G^A - G^< \Sigma^A)$ in (12) can be reordered similarly, if only the term $G^A D^<$ in $\Sigma^A \propto (GD)^A = G^A D^> - G^< D^A$ is again considered. The remaining terms $-\ G^<\ D^R$, $-\ G^<\ D^A$ from $(GD)^R$, $(GD)^A$, respectively, can also be summed to this form. Here, the imaginary part of the phonon propagator appears, instead of the electron propagator. Its real part would give further renormalization contributions, if phonon scattering was considered.

In total, the scattering shift current density $\mathbf{J_s}$ in steady state is equal to

$$\begin{aligned}
\mathbf{J}_s &= -4\, e \int \frac{d\omega}{2\pi} \int \frac{d\mathbf{k}}{(2\pi)^3} \sum_{\beta} \\
&\times \Bigg\{ \Bigg(\mathbf{R}_{s;\beta\beta}(\mathbf{k}, \mathbf{k}-\bar{\mathbf{q}})\ |M_{\beta\beta}(\mathbf{k}, \mathbf{k}-\bar{\mathbf{q}})|^2\ \mathrm{Im}\ G^R_{\beta\beta}(\mathbf{k}-\bar{\mathbf{q}}, \omega-\bar{\omega}) \\
&- \frac{1}{2}\Big(\frac{\partial\ |M_{\beta\beta}(\mathbf{k}-\bar{\mathbf{q}}, \mathbf{k})|^2}{\partial \mathbf{k}} + \frac{\partial\ |M_{\beta\beta}(\mathbf{k}-\bar{\mathbf{q}}, \mathbf{k})|^2}{\partial(\mathbf{k}-\bar{\mathbf{q}})} \Big)\ \mathrm{Re}\ G^R_{\beta\beta}(\mathbf{k}-\bar{\mathbf{q}}, \omega-\bar{\omega}) \Bigg) \\
&\times D^{>}(\bar{\mathbf{q}}, \omega-\bar{\omega})\ G^{<}_{\beta\beta}(\mathbf{k}, \omega) + \mathbf{R}_{s;\beta\beta}(\mathbf{k}, \mathbf{k}-\bar{\mathbf{q}})\ |M_{\beta\beta}(\mathbf{k}, \mathbf{k}-\bar{\mathbf{q}})|^2 \\
&\times \frac{1}{4}\Big(G^{<}_{\beta\beta}(\mathbf{k}-\bar{\mathbf{q}}, \omega-\bar{\omega}) - G^{<}_{\beta\beta}(\mathbf{k}-\bar{\mathbf{q}}, \omega+\bar{\omega}) \Big)\ G^{<}_{\beta\beta}(\mathbf{k}, \omega) \Bigg\}\,. \qquad (19)
\end{aligned}$$

The intraband correlation functions $G^{<}_{\beta\beta}$ can be obtained from the solution of the KBE similarly as in Ref.[4]. If the hot-electron population is small, then it is possible to keep in (19) only the terms linear in $G^{<}_{\beta\beta}$.

The renormalization terms in (19), with derivatives of matrix elements, give non-classical corrections to the shift current, due to *quasiparticle* broadening of the carrier spectra. Note however, that $\mathbf{J_s}$ is practically independent on the scattering rate, at least for weak scattering, since $\mathbf{R}_{s;\beta\beta}$ is determined by the crystal structure (see Appendix B), and the relaxation carrier flow is equal to the injected flow. From the same reason, the temperature dependence of $\mathbf{J_s}$ is also weak. Expression analogous to Eqn.(14), (19) can be derived for the recombination current density $\mathbf{J_r}$, but in Sec.V we argue that $\mathbf{J_r}$ is usually negligible.

4 Approximate solution for the shift currents

Here we approximate the expressions for $\mathbf{J_e}$ and $\mathbf{J_s}$ to the Boltzmann limit, which can give reasonable results in materials with a moderate scattering. First we simplify $\mathbf{J_e}$ in (14), where the light orientation is chosen along the (1,1,0) direction, appropriate in GaAs. Next, we approximate the equations for the correlation functions $G^{<}_{\beta\beta}$, and insert their solution in Eqn.(19) for $\mathbf{J_s}$, together with the shift vector $\mathbf{R}_{s;\beta\beta}$ in (B.3).

4.1 The excitation current density $\mathbf{J_e}$

In numerical studies, it is convenient to evaluate $\mathbf{J_e}$ from the expression (14) even for a linearly polarized light, so that *ab-initio* calculations of the elements $\mathbf{r}_{\beta\alpha}(\mathbf{k})$ can be performed along the usual crystal axes. Once evaluated, $\mathbf{r}_{\beta\alpha}(\mathbf{k})$ can be used to obtain the elements $\mathbf{r}_{\beta\alpha;c}(\mathbf{k})$ from the formulas (3.36-3.37) in Ref.[15]. At weak scattering, renormalization effects contained in the derivatives $\partial|r^b_{\alpha\beta}(\mathbf{k})|^2/\partial\mathbf{k}$ from Eqn.(15) can be neglected, which, in Eqn.(14), is equivalent to taking only the imaginary part of $r^a_{\beta\alpha;c}(\mathbf{k})\ r^b_{\alpha\beta}(\mathbf{k})$, anti-symmetric in the band indices. Then, $G^{<}_{vv}\ G^{A}_{cc}$ ($\alpha = v,\ \beta = c$) there can be combined with $-G^{R}_{cc}\ G^{<}_{vv}$ ($\alpha = c,\ \beta = v$),

which gives $G^<_{vv}\ (-2\ i\ \mathrm{Im}\ G^R_{cc}) = i\ A_{vv}\ A_{cc}$, where $A_{\alpha\alpha}$ are the electron spectral functions [4]. The terms with exchanged band indices are zero, since in equilibrium the conduction band is empty; *i.e.* $G^<_{cc}(\mathbf{k},\omega) = A_{cc}(\mathbf{k},\omega)\ n_{FD}(\omega) \approx 0$, where $n_{FD}(\omega) = 1/(\exp(\hbar\omega/kT)+1)$ is the Fermi-Dirac distribution.

The $\mathbf{k}$ and ω-integration in the two spectral functions $A_{vv}\ A_{cc}$ is performed as in Ref.[4]. A parabolic approximation for the bands is considered in these integrations (not in $\mathbf{r}_{\alpha\beta}(\mathbf{k})$), with wave vectors tuned to the resonant values $\mathbf{k}^n_{res}$, used to describe electrons that relax between the energy levels $E^n_{res} = E^0_{res} + n\hbar\omega_Q$ (laser tuning to E^0_{res}). The notation for angles is related to the electric field $\mathbf{E}_{\omega_0} = E_{\omega_0}/\sqrt{2}\ (1,1,0)$; the angle $\phi \in (0,\pi)$ is between the direction (1,1,0) and the $\mathbf{k}^n_{res}$-vectors, and the angle $\theta \in (0,2\pi)$ is in the plane orthogonal to the (1,1,0) direction. The nonzero z-component of the excitation current density is ($\eta = (k^0_{res},\phi,\theta)$)

$$\begin{aligned} J^z_e &= -i\ \frac{k^0_{res}e^3}{\hbar^3}\ \mu_{cv}\ |E_{\omega_0}|^2 \\ &\times \int_0^{2\pi}\frac{d\theta}{2\pi}\int_0^{\pi}\frac{d\phi}{2\pi}\ \sin(\phi)\ \Big(r^x_{cv;z}(\eta)\ r^y_{vc}(\eta) + r^y_{cv;z}(\eta)\ r^x_{vc}(\eta)\Big)\ . \end{aligned} \tag{20}$$

where $\mu_{cv} = m_c m_v/(m_c+m_v)$ is the effective electron-hole mass, and the factor in the bracket is purely imaginary. If the light polarization is in the (1,-1,0) direction, the signs at both terms with x arguments change. Since the integral is the same, the current is opposite, in agreement with Fig.1b.

4.2 The scattering current density $\mathbf{J_s}$

In order to approximate $\mathbf{J_s}$ in Eqn.(19), we need first the transport equations for the intraband correlation functions $G^<_{\beta\beta}(\mathbf{k},\omega)$. Here we describe the hot-electron relaxation by the integral KBE derived in Ref.[4]. In the weak scattering limit, they can be approximated to the integral Boltzmann equation (IBE) [4]. For simplicity, we also describe the hot carrier population only in the conduction band.

A laser light polarized along the (1,0,0) direction, used in Ref.[4], gives a nearly isotropic hot-electron distribution in the plane orthogonal to this direction, which is sufficiently described by the angle ϕ. In the present work, polarization along the $(1,1,0)$ direction gives a population squeezed in the $(0,0,1)$ direction by about 25 % (see Fig.2). Moreover, the shift vectors are also very anisotropic (see Fig.3b), so that both angular variables ϕ, θ must be used. The field self-energy for *interband* transitions along the (1,1,0) direction can be obtained from the expression (10) in the form

$$\Sigma^+_{f;cv}(\phi,\theta) = -e\ \Big(r^x_{cv}(k^0_{res},\phi,\theta) + r^y_{cv}(k^0_{res},\phi,\theta)\Big)\ E_{\omega_0}/\sqrt{2}\ . \tag{21}$$

In the scattering self-energy $\Sigma_{s;cc}$, the matrix elements $M_{cc}(\mathbf{k},\mathbf{k}')$ use the linearized structure factors $\gamma_{cc}(\mathbf{k},\mathbf{k}')$ from (B.10). Since *intraband* relaxation is considered, the

square of the exponential prefactor from (B.10) gives $\gamma_{cc}(\mathbf{k},\mathbf{k}^{'}) \approx 1$, *i.e.* $M_{cc}(\mathbf{k},\mathbf{k}^{'}) = M(\mathbf{k}-\mathbf{k}^{'})$ from (5).

Then using the steps in Ref.[4], we arrive at the steady-state IBE

$$f_{cc}(n,\phi,\theta) = \frac{2\ k^n_{res}\ \tau_o(n)}{\hbar^3}\ \Big\{ |\Sigma^+_{f;cv}(\phi,\theta)|^2\ \mu_{cv}\ \delta_{n0} + \frac{m_c}{2}\ M_0^2\ \int_0^{2\pi}\frac{d\bar{\theta}}{2\pi}\ \int_0^{\pi}\frac{d\bar{\phi}}{2\pi}\ \sin(\bar{\phi})\ \Big(\frac{1}{|\mathbf{k}^n_{res}-\bar{\mathbf{k}}^{n-1}_{res}|^2}\ f_{cc}(n-1,\bar{\phi},\bar{\theta})\ n_B(\omega_Q) + \frac{1}{|\mathbf{k}^n_{res}-\bar{\mathbf{k}}^{n+1}_{res}|^2}\ f_{cc}(n+1,\bar{\phi},\bar{\theta})\ (1+n_B(\omega_Q))\Big)\Big\}\ , \tag{22}$$

where the distribution function on the n-th level ($\varepsilon^{\pm}_n = E^n_{res} \pm n\hbar\omega_Q/2$)

$$f_{cc}(n,\phi,\theta) = \int_{\varepsilon^-_n}^{\varepsilon^+_n}\frac{d\hbar\omega}{2\pi}\ \int_0^{\infty}\frac{dk}{2\pi}\ k^2\ G^{<}_{2;cc}(k,\phi,\theta,\omega) \tag{23}$$

is defined from the second order $G^{<} \approx G^{<}_2/2!$, expanded in terms of the interband field self-energy $\Sigma_{f;cv}$; the prefactor 2 in Eqn.(22) cancels this 2!. Here $\tau_o(n) = -\hbar/(2\ \mathrm{Im}\Sigma^r_{cc,s}(n))$ is the particle relaxation time. It is still necessary to add in Eqn.(22) radiative transfers of carriers between the bands, but this is practically not reflected in $\mathbf{J_e}$, and $\mathbf{J_r}$ is also negligible.

To calculate $\mathbf{J_s}$, we also need a simpler expression for the scattering shift vector $\mathbf{R}_{s;\beta\beta}(\mathbf{k},\mathbf{k}^{'})$ in (B.4). A tractable approximation [9, 10] can be obtained if this is linearized in terms of the wave vector difference $\mathbf{k}-\mathbf{k}^{'}$, around the center $\mathbf{k}_0 = (\mathbf{k}^{'}+\mathbf{k})/2$. For large differences, where the errors can grow, the contributions to scattering are small, since the elements $|M(\mathbf{k}-\mathbf{k}^{'})|^2$ decay as $|\mathbf{k}-\mathbf{k}^{'}|^{-2}$. Direct algebraic manipulation gives the scattering shift vector in (B.11-B.12). In the current formula (19), we expand the vector $\mathbf{R}_{s;\beta\beta}$ in each *considered* wave vector $\mathbf{k}$ in the Brillouin zone.

Finally, the expression (19) for $\mathbf{J}_s$ can be rewritten in the Boltzmann limit, where $A_{\beta\beta}(\mathbf{k},\omega) = -2\ \mathrm{Im}\ G^R_{\beta\beta}(\mathbf{k},\omega) \approx 2\pi\delta(\hbar\omega - \epsilon_\beta(\mathbf{k}))$. Since the correlation function $D^{>}(\mathbf{q},\omega)$ for free phonons is also sharp, it can be easily convoluted over frequency and momentum with $A_{\beta\beta}(\mathbf{k},\omega)$. If we consider in (19) only the term linear in $G^{<}_{\beta\beta}$, and neglect renormalization factors, then the approximate $\mathbf{J}_{s;cc}$ results

$$\begin{aligned}\mathbf{J}_{s;cc} &= -\frac{e\ m_c\ M_0^2}{\hbar^2}\ \sum_n \int_0^{2\pi}\frac{d\theta}{2\pi}\ \int_0^{\pi}\frac{d\phi}{2\pi}\ \sin(\phi)\ f_{cc}(n,\phi,\theta) \\ &\times \int_0^{2\pi}\frac{d\bar{\theta}}{2\pi}\ \int_0^{\pi}\frac{d\bar{\phi}}{2\pi}\ \sin(\bar{\phi})\ \Big(\frac{k^{n-1}_{res}}{|\mathbf{k}^n_{res}-\bar{\mathbf{k}}^{n-1}_{res}|^2}\ (\mathbf{k}^n_{res}-\bar{\mathbf{k}}^{n-1}_{res}) \times \mathbf{\Omega}_c(\mathbf{k}^n_{res})\ (1+n_B(\omega_Q)) \\ &+ \frac{k^{n+1}_{res}}{|\mathbf{k}^n_{res}-\bar{\mathbf{k}}^{n+1}_{res}|^2}\ (\mathbf{k}^n_{res}-\bar{\mathbf{k}}^{n+1}_{res}) \times \mathbf{\Omega}_c(\mathbf{k}^n_{res})\ n_B(\omega_Q)\Big)\ . \end{aligned} \tag{24}$$

Here the distribution from (23) has been used, where the integration over ω and $k = |\mathbf{k}|$ from (19) is already performed. A more consistent approximation in Eqn.(24) can

be obtained by evaluating the vectors $\mathbf{\Omega}_c$ at the points $(\mathbf{k}^n_{res} + \bar{\mathbf{k}}^{\pm 1}_{res})/2$. Numerically, it is easier to average $\mathbf{\Omega}_c$, evaluated at the side points $\mathbf{k}^n_{res}$, $\bar{\mathbf{k}}^{\pm 1}_{res}$.

5 Numerical results and discussions

In applications, we consider a typical experimental configuration for GaAs; the laser intensity is $I = 10^6$ W/cm^2 at the light energy $\hbar\omega_0 = 2.1$ eV (band gap $E_g = 1.5$ eV), with light polarized along the (1,1,0) direction. We calculate the steady-state $\mathbf{J_e}$ from Eqn.(20), and $\mathbf{J_s}$ is obtained by solving Eqn.(22) for the intraband distribution $f_{\beta\beta}(n, \phi, \theta)$, which is then used in Eqn.(24). The recombination current density $\mathbf{J_r}$ is also discussed.

We consider a model of GaAs with 10 bands, without spin-orbit coupling. The matrix elements $\mathbf{r}_{ij}$ are calculated *ab initio* within the density functional theory in local density approximation using a plane wave-pseudopotential approach [26]. They are obtained at the resonant momentum k^0_{res} (resonant value for the light energy $\hbar\omega_0$) and at about 40 energy (momentum) levels in the band c, corresponding to resonant values of LO phonon processes (E^n_{res} at momenta k^n_{res}). The elements are found on a mesh (ϕ_i, θ_j), which can be reduced due to symmetry to a size 10×20 points in the region $\phi = (0, \pi/2)$, $\theta = (0, \pi)$, giving in total around 100 Mb of input data. The calculated current density $\mathbf{J_e}$ corresponds to the excitation between the heavy hole bands ($v = 3, 4$ in Eqn.(21)) and the lowest conduction band ($c = 5$), while $\mathbf{J_s}$ is illustrated only in the band $c = 5$.

5.1 The electron distributions

In Fig.2, we show cross sections, orthogonal to the (1,1,0) direction, through the electron population $f_{cc}(n, \phi, \theta)$ in the conduction band, multiplied by $\sin(\phi)$ as in Eqn.(24). The solid and four dashed lines on each plot correspond to the angles $\phi = i\ \pi/10$ ($i = 5 - 1$), while the shapes of the ovals give the θ-distribution. The presented levels are $n = 0, -1, -2$, and the temperature is $T = 300$ K. Note, that the population ($n = 0$) is squeezed in the (0,0,1) and (1,1,0) directions, where the last is seen on the fast decays with ϕ of the ovals for $n = 0$. The population squeezed in the plane orthogonal to the (1,1,0) direction, around $\phi \approx 0$, contributes more to the shift current than the population in the plane orthogonal to the (1,-1,0) direction. Therefore, these contributions with opposite signs do not cancel, and J^z_e can be nonzero. For a light polarized in the (1,-1,0) direction, the population is squeezed in the orthogonal direction, according to the change in $|r^x_{cv} \pm r^y_{cv}|^2$ from (21), and J^z_e changes sign. At lower levels both squeezing become relaxed, which visually shrinks the size of the population. Relaxation of anisotropy in hot carrier distributions was also studied in Ref.[27].

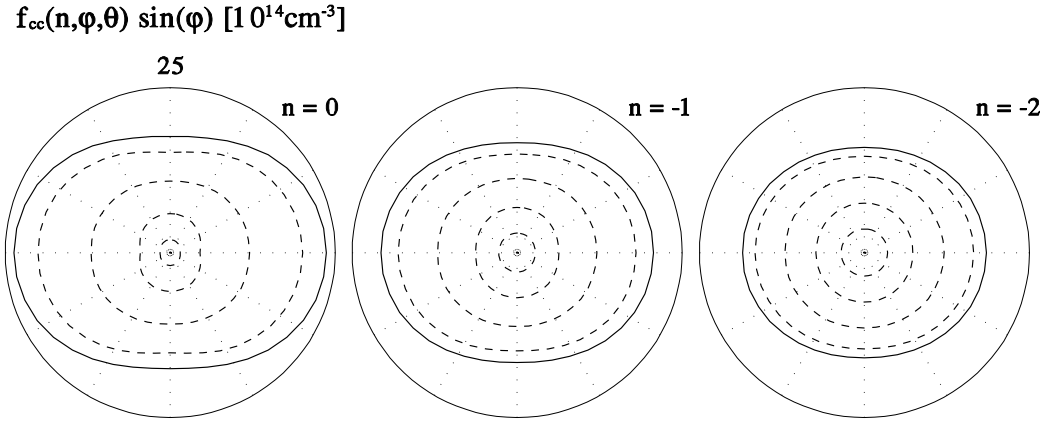

Figure 2: Crossections through the population $f_{cc}(n, \phi, \theta)$, multiplied by $\sin(\phi)$, in the planes orthogonal to the (1,1,0) direction. The values for levels $n = 0, -1, -2$ show relaxation of the squeezing along the (0,0,1) and (1,1,0) directions. The solid and four dashed lines correspond to the angles $\phi = i\ \pi/10$ $(i = 5 - 1)$.

5.2 The shift current density $\mathbf{J_e}$

In Fig.3a, we show the angular dependence of $\Delta_{rr} = \mathrm{Im}\ (r^x_{cv;z}\ r^y_{vc} + r^y_{cv;z}\ r^x_{vc})$, multiplied by $\sin(\phi)$, from the expression (20) for $\mathbf{J_e}$. It is calculated for the angles as in Fig.2, and for the light polarized in the (1,1,0) direction. If the light is polarized in the (1,-1,0) direction, Δ_{rr} looks the same, but the prefactor in Eqn.(20) changes sign. This reflects the fact that the structure of GaAs allows pumping from different atoms in both situations, but it gives $\mathbf{J_e} = 0$ for excitation by unpolarized light. For the present excitation, we obtain from Eqn.(20) the value $J^z_e \approx -45$ A/cm^2. This agrees in sign with Fig.1b (negative charge of electrons) and in value with Ref.[16].

5.3 The scattering current density $\mathbf{J_s}$

Evaluation of $\mathbf{J_s}$ is sensitive to numerical errors, resulting from approximate integrations on the finite mesh for ϕ, θ. We have corrected three problems in the calculation of $\mathbf{J}_{s;cc}$. First, it is the flow between level n and $n \pm 1$, second the conservation of homogeneous distributions (used as an initial test) in scattering between level n and $n \pm 1$, and third the fact that nonzero shift currents might result even for homogeneous distributions, which is a non-physical consequence of the rough mesh and other approximations.

In Fig.3b, we show the z-component of the linearized scattering shift vector $R^z_{s;cc}$ from the level $n = 0$; the cross section is orthogonal to the (1,1,0) direction at $\phi = \pi/2$. The behavior of $R^z_{s;cc}$ can be appreciated, if we substitute the difference of wave vectors in (B.11-B.12) by $-\mathbf{k}$. This because, in average, the wave vector $\mathbf{k}$ of the excited electron becomes scattered in the $-\mathbf{k}$ direction, even though the size k^0_{res} of $-\mathbf{k}$ is about an order of magnitude larger than the difference $k^0_{res} - k^{\pm 1}_{res}$. The

vector $R^z_{s;cc}$ changes a sign, if the cross section is orthogonal to the (1,-1,0) direction, proving zero current for a homogeneous distribution. Because of the symmetry specified above, we can limit calculations to one quarter of the Brillouin zone. Note that $R^z_{s;cc}$ is larger in the horizontal direction, where the squeezed population in Fig.2 is also larger, so that $J^z_{s;cc}$ becomes increased.

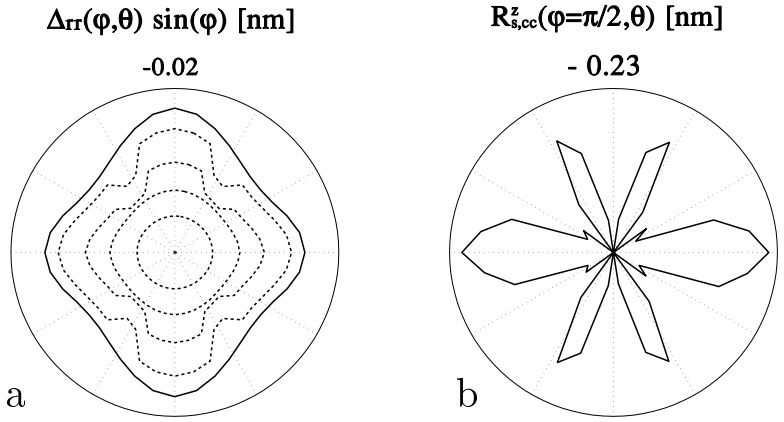

Figure 3: Inset a) shows the angular dependence of the factor $\Delta_{rr} = \mathrm{Im}\left(r^x_{cv;z}\ r^y_{vc} + r^y_{cv;z}\ r^x_{vc}\right)$, multiplied by $\sin(\phi)$, calculated from the level $n = 0$. The crossections are in the plane orthogonal to the polarization direction of light (1,1,0). It is opposite if light is polarized in the direction (1,-1,0). This proves the mechanism in Fig.1b, with zero current J^z_e for excitation by unpolarized light. In the inset b) we present the approximate scattering shift vector $R^z_{s;cc}(\phi = \pi/2, \theta) \approx (-\mathbf{k} \times \mathbf{\Omega}_c)^z$, calculated from the level $n = 0$. The crossection is as in inset a). For the orthogonal crossection, the contributions only change sign. Thus $J^z_{s;cc} = 0$ for homogeneous electron distribution, resulting approximately for excitation by unpolarized light.

In Fig.4a, we present contributions to $J^z_{s;cc}$ from different electron levels in the conduction band, as induced by phonon scattering [4]. The temperature is $T = 300$ K, and the dashed, solid and dash-dotted lines correspond to the light excitation at the energies corresponding to the levels $n = -2, 0, 2$ (used the same injection rate). The three results are very different, since the shift vector $R^z_{s;cc}$ and, consequently, $J^z_{s;cc}$ changes sign around level $n = 0$ (see also Fig.5). This effect is related to the form of matrix elements, and it appears by chance close to the level $n = 0$.

The contributions to the current density $J^z_{s;cc}$ are summed and presented in Fig.4b in the range $T = 50 - 300$ K. The excitation energies are labeled by the level number $n = 0, 5, 10$. In this interval the response changes sign, as expected from Fig.4a. $J^z_{s;cc}$ is about 3 orders of magnitude smaller than J^z_e, but it increases for larger excitation energies (see Fig.5). For excitation around $n = 0$, $J^z_{s;cc}$ is nearly temperature independent, while away from $n = 0$ it grows in size with T. In general the increase is small, since $J^z_{s;cc}$ depends weakly on the scattering strength (see discussion at Eqn.(19)).

In Fig.5, we show the dependence of the ratio $J^z_{s;cc}/J^z_e$ on the excitation energy, labeled as in Fig.4b. As already mentioned, the ratio is negative close to the Γ point,

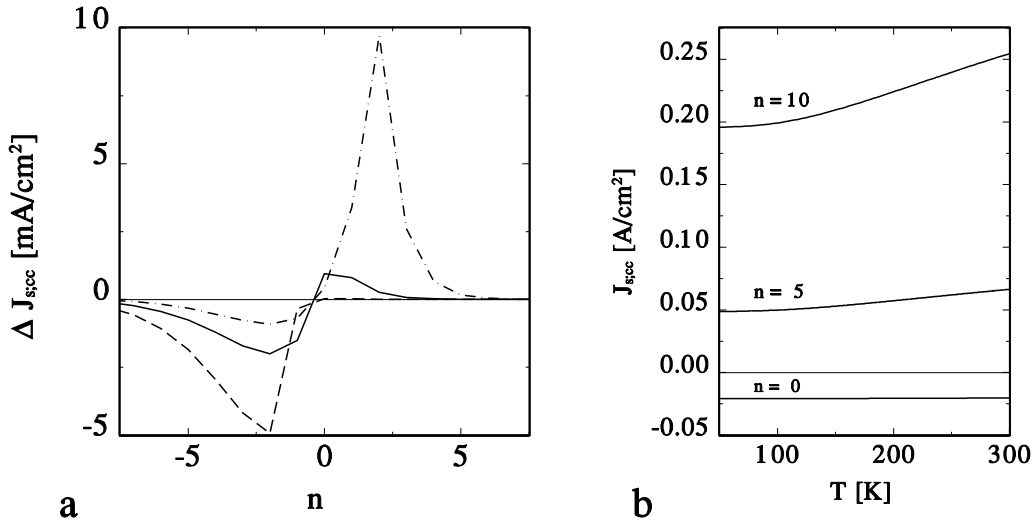

Figure 4: Inset a) shows contributions to the scattering shift current density $J^z_{s;cc}$ from different "electron levels", due to scattering on LO phonons at $T = 300$ K. The dashed, solid and dot-dashed lines correspond to tuning the laser to the energy of the level $n = -2, 0, 2$. The change of sign of the contributions is due to the fact that $R^z_{s;cc}$ at angles $\phi = \pi/2$ changes sign at these excitation energies. In inset b) we present the temperature dependence of the scattering shift current density $J^z_{s;cc}$ calculated as a sum of its components in inset a). The situations correspond to tuning the laser energy on the levels $n = 0, 5, 10$. $J^z_{s;cc}$ changes sign and slightly increases with temperature, especially at larger n.

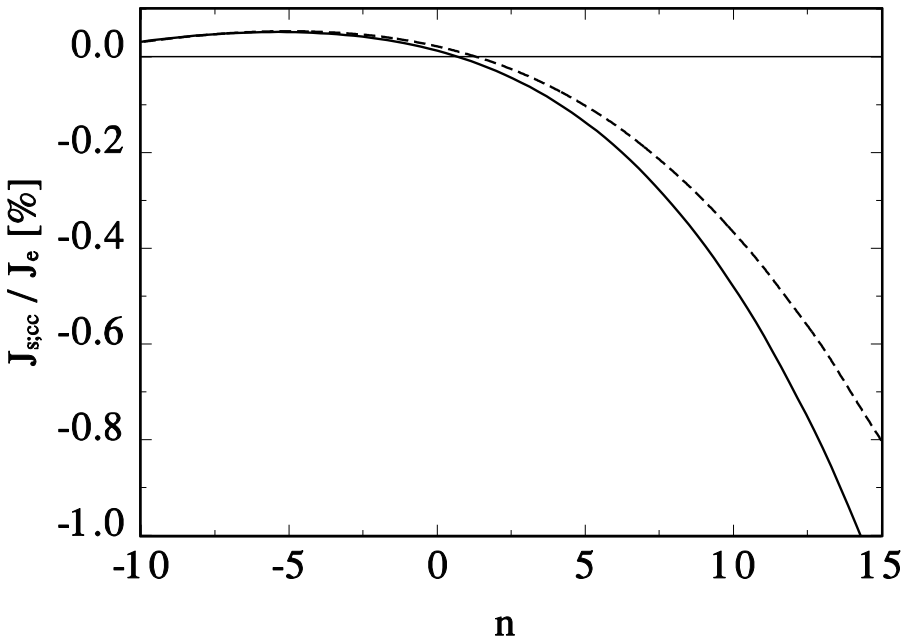

Figure 5: Ratio of the scattering and excitation shift current densities $J_{s;cc}/J_e$, calculated as a function of excitation energy, labeled in phonon levels. The solid (dashed) lines correspond to $T = 300$ K ($T = 50$ K). The ratio changes sign around $n = 0$ from positive to negative and increases in value up to 1% for the present excitation energies.

it changes sign around $n = 0$ and approaches 1 % at $n = 15$. Here we stop our calculations, since the departure from the parabolic band approximation is large. The solid (dashed) curves correspond to $T = 300$ K ($T = 50$ K). Since J_e^z roughly increases by 25% in this energy region, $J_{s;cc}^z$ is responsible for the increased value in the ratio. Note also that at higher excitation energies the current density $J_{s;cc}^z$ is *opposite* to J_e^z, which could be intuitively expected. The ratio can be larger for relaxation to/from local side minima in the band structure.

5.4 The recombination current density $\mathbf{J_r}$

Finally, let us shortly discuss the recombination current density $\mathbf{J_r}$. Since the momentum relaxation time τ_p is several hundreds fs, and the recombination time τ_r is about 1 ns, only a tinny fraction of carriers recombine before randomizing their momenta. The hot carriers first isotropically fill the Brillouin zone, and in particular the distribution is practically the same in the (1,1,0) and (1,-1,0) directions. It is good to recognize that $\mathbf{J_e}$ and $\mathbf{J_r}$ resulting from transitions between two particular states have opposite signs. Therefore, contributions to $\mathbf{J_r}$ from the population in the above directions are the same in magnitude, but they point in the (0,0,-1) and (0,0,1) directions. This means that $\mathbf{J_r}$ is practically zero, as suggested in Fig.1b, where the recombining electrons going from Ga atoms do not distinguish between the As atoms. The same observation is expressed in Ref.[1] in a more general way, namely, that $\mathbf{J_r}$ is zero in non-pyroelectric materials.

Recombination through trap sites from impurities would give nonzero *microscopic* shift currents, but its macroscopic value $\mathbf{J_r}$ averaged over all impurity positions should be negligible. It would be also interesting to study the shift current related with transitions to excitonic levels. Since these levels are energetically below the band edge, it can be expected that they give different (smaller) shifts in real space than in the interband transitions. These shifts would also vary level from level, and $\mathbf{J_r}$ could be also nonzero.

6 Conclusion

We have theoretically investigated laser beam generation of the shift current density in bulk NCS semiconductors. The excitation, scattering and recombination components $\mathbf{J_{e,s,r}}$ reflect *asymmetric carrier flows* in elementary cells, induced by the relevant processes. The system was described by the NGF methods, which, in combination with the length gauge, gives a consistent approach to this problem. Expressions for $\mathbf{J_{e,s}}$ were derived for steady-state excitations, in terms of the carrier transition rates and the space shift vectors $\mathbf{R_{e,s}}$.

For practical purposes, we have simplified the formalism to the Boltzmann

limit and demonstrated a tractable numerical scheme. Within this approximation, we have described optically excited GaAs in the presence of LO phonon scattering. Light induced electron transitions between the lowest conduction band and the nearest heavy hole bands were considered. For light polarized in the (1,1,0) direction, the excitation current density $\mathbf{J_e}$ in the (0,0,-1) direction was obtained. The scattering current density $\mathbf{J_{s;cc}}$ was calculated from the hot-electron distribution in the conduction band. It is about two orders of magnitude smaller than $\mathbf{J_e}$, and the recombination current density $\mathbf{J_r}$ can be neglected, since the momentum relaxation causes that electrons recombine with the same strength to atoms placed in opposite directions. Therefore, *steady-state pumping* of electrons across the crystal can be realized.

The shift current has potential applications in ultrafast photo-electric devices, since the response is practically instantaneous. Modifications of the shift current might be observed in low dimensional structures, heteropolar nanotubes [28] or molecular systems.

Acknowledgments

The author would like thank J. E. Sipe for many discussions of the problem studied and a financial support provided by Photonic Research Ontario. He acknowledges B. Adolf and A. Shkrebtii for evaluation of *ab-initio* matrix elements. The work was greatly improved with the help of K. Busch and with comments of A. P. Jauho.

Appendix A

Let us first compare current expressions from Ref.[16] with our results. The sum of the term $\langle J^a_{intra}\rangle^I$ and $d\ \langle \mathbf{P}^{(2)}_{inter}\rangle/dt$, there, corresponds to the excitation shift current density $\mathbf{J_e}$ from our Eqn.(12), if scattering is neglected. The term $\langle J^a_{intra}\rangle^{II}$ there corresponds to the excitation part of the ballistic current; Eqn.(12) with equal bands $\alpha = \beta$, and no transport vertex corrections to $G^<_{\alpha\alpha}$.

Next, we show how Eqn.(14) can be obtained from Eqn.(13), in analogy to Ref.[16]. Two situations can be considered in (13), where either one of the two involved field self-energies $\Sigma^{\pm}_{f;\alpha\beta}$ is interband and the other is intraband, or both of them are interband. In the first case, the *interband* self-energy in Eqn.(13) is between the two Green functions, since these are from different bands (empty/full), to give real transitions. The *intraband* self-energy in front or back can be switched by partial integration (see comment at (9)) to give a derivative, with a prefactor 1, over the front or back variable in the first or second term in Eqn.(13) with $G^<_{1;\alpha\beta}$. These two can be combined into a derivative $\partial G^<_{1;\alpha\beta}(\mathbf{k},\mathbf{k})/\partial\mathbf{k}$, and transferred by partial integration to the derivative in the prefactor [16] $-\partial\mathbf{r}_{\alpha\beta}(\mathbf{k})/\partial\mathbf{k}$. The resulting

contribution to $\mathbf{J_e}$ in (13) is

$$\Delta\mathbf{J_e} = 2ie^3 \int \frac{d\omega}{2\pi} \int \frac{d\mathbf{k}}{(2\pi)^3} \sum_{\alpha\neq\beta} (-i\ \mathbf{r}_{\beta\alpha;a}(\mathbf{k})\ r^b_{\alpha\beta}(\mathbf{k}))\ E^a_{\mp\omega_0}\ E^b_{\pm\omega_0} \times \Big(G_{0;\alpha\alpha}(\mathbf{k},\omega)\ G_{0;\beta\beta}(\mathbf{k},\omega\pm\omega_0) \Big)^< , \tag{A.1}$$

where we employ the definition [16]

$$\mathbf{r}_{\beta\alpha;a}(\mathbf{k}) = \frac{\partial \mathbf{r}_{\beta\alpha}(\mathbf{k})}{\partial k^a} - i\ (\xi^a_{\beta\beta}(\mathbf{k}) - \xi^a_{\alpha\alpha}(\mathbf{k}))\ \mathbf{r}_{\beta\alpha}(\mathbf{k})\ . \tag{A.2}$$

In (A.1) the sum over bands $\alpha \neq \beta$ selects real transitions between valence and conduction bands, tuned by the laser frequency ω_0. Then, the top (bottom) signs correspond to $\alpha = c$, $\beta = v$ ($\alpha = v$, $\beta = c$).

The second situation adds the expression $\mathbf{r}_{\beta\alpha}(\mathbf{k})\ \sum_{\gamma\neq\alpha,\beta}\ [\xi^a_{\alpha\gamma}(\mathbf{k})\ \xi^b_{\gamma\beta}(\mathbf{k}) - \xi^b_{\alpha\gamma}(\mathbf{k})\ \xi^a_{\gamma\beta}(\mathbf{k})]$ to the bracket $(-i\ \mathbf{r}_{\beta\alpha;a}(\mathbf{k})\ \xi^b_{\alpha\beta}(\mathbf{k}))$ in (A.1). These terms can be largely simplified with the following identity [16]

$$r^a_{\alpha\beta;b}(\mathbf{k}) - r^b_{\alpha\beta;a}(\mathbf{k}) = i \sum_{\gamma\neq\alpha,\beta} [\xi^b_{\alpha\gamma}(\mathbf{k})\ \xi^a_{\gamma\beta}(\mathbf{k}) - \xi^a_{\alpha\gamma}(\mathbf{k})\ \xi^b_{\gamma\beta}(\mathbf{k})]\ , \tag{A.3}$$

which can be used to exchange the vector (b) and derivative (a) components in $r^b_{\alpha\beta;a}(\mathbf{k})$. If we substitute (A.3) in (A.1), and shift arguments, then the square brackets cancel and the expression (14) results.

Appendix B

Here we derive the expression for the intraband scattering shift vector $\mathbf{R}_{s;\beta\beta}(\mathbf{k},\mathbf{k}')$, used in Eqn.(19), and linearize it in the wave vector difference $\mathbf{k}-\mathbf{k}'$.

We assume [9, 10] that the commutator of the operator $\mathbf{x}$ in (2) and $\mathbf{M}$ in (5) vanishes, *i.e*, $[\mathbf{x},\mathbf{M}] = 0$. In the Bloch representation, we can easily sum over intermediate states and momenta. Upon separating out the terms of the position operator that are band-diagonal, we arrive at the following sum rule:

$$\begin{aligned} &\sum_{\alpha\neq\beta} \mathbf{r}_{\beta\alpha}(\mathbf{k})\, M_{\alpha\gamma}(\mathbf{k},\mathbf{k}') - \sum_{\alpha\neq\gamma} M_{\beta\alpha}(\mathbf{k},\mathbf{k}')\, \mathbf{r}_{\alpha\gamma}(\mathbf{k}') \\ &= -i\left(\frac{\partial}{\partial\mathbf{k}} + \frac{\partial}{\partial\mathbf{k}'}\right) M_{\beta\gamma}(\mathbf{k},\mathbf{k}') + M_{\beta\gamma}(\mathbf{k},\mathbf{k}') \Big(\xi_{\gamma\gamma}(\mathbf{k}') - \xi_{\beta\beta}(\mathbf{k})\Big)\ . \end{aligned} \tag{B.1}$$

Aided with Eqn.(B.1) and writing the matrix elements $M_{\beta\beta}(\mathbf{k},\mathbf{k}')$ in the form

$$M_{\beta\beta}(\mathbf{k},\mathbf{k}') = |M_{\beta\beta}(\mathbf{k},\mathbf{k}')|\ e^{i\phi_{\beta\beta}(\mathbf{k},\mathbf{k}')}\ , \tag{B.2}$$

it is now straightforward to simplify the bracketed terms in Eqn.(18) for $\gamma = \beta$:

$$\Big(\sum_{\alpha\neq\beta} r^c_{\beta\alpha}(\mathbf{k})\ M_{\alpha\beta}(\mathbf{k},\mathbf{k}') - \sum_{\beta\neq\alpha} M_{\beta\alpha}(\mathbf{k},\mathbf{k}')\ r^c_{\alpha\beta}(\mathbf{k}')\Big)\ M_{\beta\beta}(\mathbf{k}',\mathbf{k})$$

$$= \quad R^c_{s;\beta\beta}(\mathbf{k},\mathbf{k}^{'})\ |M_{\beta\beta}(\mathbf{k}^{'},\mathbf{k})|^2 - \frac{i}{2}\left(\frac{\partial}{\partial k^c}+\frac{\partial}{\partial k'^c}\right)|M_{\beta\beta}(\mathbf{k}^{'},\mathbf{k})|^2\ . \qquad \text{(B.3)}$$

Here the c-component of the scattering shift vector $\mathbf{R}_{s;\beta\beta}(\mathbf{k},\mathbf{k}^{'})$ is

$$R^c_{s;\beta\beta}(\mathbf{k},\mathbf{k}^{'}) = \left(\frac{\partial}{\partial k^c}+\frac{\partial}{\partial k'^c}\right)\phi_{\beta\beta}(\mathbf{k},\mathbf{k}^{'}) + \xi^c_{\beta\beta}(\mathbf{k}^{'}) - \xi^c_{\beta\beta}(\mathbf{k})\ . \qquad \text{(B.4)}$$

It has properties similar to the excitation shift vector $\mathbf{R}_{e;\alpha\beta}(\mathbf{k})$ in (16). $\mathbf{R}_{s;\beta\beta}(\mathbf{k},\mathbf{k}^{'})$ is invariant under phase transforms of Bloch functions, and anti-symmetric upon exchanging $\mathbf{k}$ and $\mathbf{k}^{'}$, *i.e.* $\mathbf{R}_{s;\beta\beta}(\mathbf{k},\mathbf{k}^{'}) = -\mathbf{R}_{s;\beta\beta}(\mathbf{k}^{'},\mathbf{k})$, which follows directly from Eqn.(B.2). Therefore, the real (first) part in Eqn.(B.3) is also anti-symmetric, while the imaginary (second) part is symmetric, and these two give different contributions to the scattering shift current density $\mathbf{J}_s$.

Numerically, it is more convenient to evaluate the shift vector directly from from the matrix elements $M_{\alpha\beta}(\mathbf{k},\mathbf{k}^{'})$, which are accessible to *ab-initio* calculations. Then, considerable care has to be exerted in order to maintain the invariance under phase transformations. We make use of the specific form of $M_{\beta\beta}(\mathbf{k},\mathbf{k}^{'})$, with the structure factors $\gamma_{\beta\beta}(\mathbf{k},\mathbf{k}^{'})$ given in Eqn.(5), to evaluate $R^c_{s;\beta\beta}(\mathbf{k},\mathbf{k}^{'})$ from

$$\begin{aligned} R^c_{s;\beta\beta}(\mathbf{k},\mathbf{k}^{'}) \quad &= \quad \mathrm{Im}\left[\frac{1}{|\,\gamma_{\beta\beta}(\mathbf{k},\mathbf{k}')\,|^2}\,\gamma^*_{\beta\beta}(\mathbf{k},\mathbf{k}^{'})\left(\frac{\partial}{\partial k^c}+\frac{\partial}{\partial k'^c}\right)\gamma_{\beta\beta}(\mathbf{k},\mathbf{k}^{'})\right] \\ &+ \quad \xi^c_{\beta\beta}(\mathbf{k}^{'}) - \xi^c_{\beta\beta}(\mathbf{k})\ . \end{aligned} \qquad \text{(B.5)}$$

Since $\gamma_{\beta\beta}(\mathbf{k},\mathbf{k}^{'})$ only depends on the band structure, it is clear that the shift vector $R^c_{s;\beta\beta}$ is an *intrinsic property of the material* and does not depend on the nature of the scattering mechanism.

Eqn.(B.5) can be used once $\gamma_{\beta\beta}(\mathbf{k},\mathbf{k}^{'})$ are found. For practical evaluations it is much easier to obtain their linearized form in the difference $\mathbf{k}-\mathbf{k}^{'}$. We can evaluate $u_{\beta\mathbf{k}}(\mathbf{x})$ and $u_{\beta\mathbf{k}'}(\mathbf{x})$ as well as their derivatives from $u_{\beta\mathbf{k}_0}(\mathbf{x})$ at $\mathbf{k}_0 = (\mathbf{k}+\mathbf{k}^{'})/2$ using **kp**-perturbation theory [29]. This allows us to obtain corresponding perturbation theoretical expressions for $\gamma_{\beta\beta}(\mathbf{k},\mathbf{k}^{'})$, $\xi_{\beta\beta}(\mathbf{k})$ and the shift vector $R^c_{s;\beta\beta}(\mathbf{k},\mathbf{k}^{'})$.

The linearized $u_{\beta\mathbf{k}}(\mathbf{x})$ results in the form

$$u_{\beta\mathbf{k}_0+\Delta\mathbf{k}}(\mathbf{x}) = e^{-i\xi_{\beta\beta}(\mathbf{k}_0)\cdot\Delta\mathbf{k}}\left(u_{\beta\mathbf{k}_0}(\mathbf{x}) - i\,\Delta\mathbf{k}\cdot\sum_{\alpha\neq\beta}\mathbf{r}_{\alpha\beta}(\mathbf{k}_0)\,u_{\alpha\mathbf{k}_0}(\mathbf{x})\right)\ , \qquad \text{(B.6)}$$

where $\Delta\mathbf{k} = \mathbf{k}-\mathbf{k}_0$. The exponential prefactor reflects the change of the phase in the Bloch wave $u_{\beta\mathbf{k}_0+\Delta\mathbf{k}}(\mathbf{x})$, which is otherwise completely undetermined. As mentioned above, this phase is of paramount importance, since we have to take derivatives with respect to $\mathbf{k}$ from the Bloch wave $u_{\beta\mathbf{k}_0+\Delta\mathbf{k}}(\mathbf{x})$ (see Eqn.(B.5)). Therefore, we have to consider *all* $\mathbf{k}$ dependencies of $u_{\beta\mathbf{k}_0+\Delta\mathbf{k}}(\mathbf{x})$ to ensure phase transformation invariance of our results. In addition, it follows directly from Eqn.(B.6) that

$$\frac{\partial u_{\beta\mathbf{k}}(\mathbf{x})}{\partial\mathbf{k}} = -i\ \xi_{\beta\beta}\ u_{\beta\mathbf{k}}(\mathbf{x}) - i\sum_{\alpha\neq\beta}\mathbf{r}_{\alpha\beta}(\mathbf{k})\,u_{\alpha\mathbf{k}}(\mathbf{x})\ , \qquad \text{(B.7)}$$

which is consistent with Eqn.(3), since the fast component of Bloch functions $u_{\alpha\mathbf{k}}(\mathbf{x})$ and $u^*_{\beta\mathbf{k}}(\mathbf{x})$ are orthogonal in the unit cell.

Using in Eqn.(B.5) the derivative of the expression (5), done with the help of Eqn.(B.7), gives the exact result

$$\begin{aligned} R^c_{s;\beta\beta}(\mathbf{k},\mathbf{k}') &= \frac{1}{|\gamma_{\beta\beta}(\mathbf{k},\mathbf{k}')|}\ \mathrm{Im}\ \left[\ i\ \gamma^*_{\beta\beta}(\mathbf{k},\mathbf{k}')\ \rho^c_{s;\beta\beta}(\mathbf{k},\mathbf{k}')\ \right]\ , \\ \rho^c_{s;\beta\beta}(\mathbf{k},\mathbf{k}') &= \sum_{\alpha\neq\beta}\Big(r^c_{\beta\alpha}(\mathbf{k})\ \gamma_{\alpha\beta}(\mathbf{k},\mathbf{k}') - \gamma_{\beta\alpha}(\mathbf{k},\mathbf{k}')\ r^c_{\alpha\beta}(\mathbf{k}')\Big)\ . \end{aligned} \tag{B.8}$$

Eqn.(B.6) may now be used to obtain the **kp**-perturbation expression for $\mathbf{r}_{\beta\alpha}(\mathbf{k})$

$$\begin{aligned} \mathbf{r}_{\beta\alpha}(\mathbf{k}) &= e^{i(\xi_{\beta\beta}(\mathbf{k}_0)-\xi_{\alpha\alpha}(\mathbf{k}_0))\cdot\Delta\mathbf{k}} \\ &\times \left(\mathbf{r}_{\beta\alpha}(\mathbf{k}_0) + \sum_{\gamma\neq\beta}\sum_{\sigma\neq\alpha}(\Delta\mathbf{k}\cdot\mathbf{r}_{\beta\gamma}(\mathbf{k}_0))\ \mathbf{r}_{\sigma\alpha}(\mathbf{k}_0)\ \delta_{\gamma\sigma}\right)\ . \end{aligned} \tag{B.9}$$

Similarly can be obtained the expression for $\gamma_{\beta\alpha}(\mathbf{k},\mathbf{k}')$

$$\begin{aligned} \gamma_{\beta\alpha}(\mathbf{k},\mathbf{k}') &= e^{i(\xi_{\beta\beta}(\mathbf{k}_0)\cdot\Delta\mathbf{k}-\xi_{\alpha\alpha}(\mathbf{k}_0)\cdot\Delta\mathbf{k}')} \\ &\times \left(\delta_{\beta\alpha} - i\ \Delta\mathbf{k}\cdot\sum_{\sigma\neq\alpha}\mathbf{r}_{\sigma\alpha}(\mathbf{k}_0)\ \delta_{\beta\sigma} + i\ \Delta\mathbf{k}'\cdot\sum_{\beta\neq\sigma}\mathbf{r}_{\beta\sigma}(\mathbf{k}_0)\ \delta_{\sigma\alpha}\right) \end{aligned} \tag{B.10}$$

where $\Delta\mathbf{k} = \mathbf{k} - \mathbf{k}_0$, $\Delta\mathbf{k}' = \mathbf{k}' - \mathbf{k}_0$. Upon inserting these results in the expression (B.8) and making use of the vector identity $\mathbf{a}\times(\mathbf{b}\times\mathbf{c}) = \mathbf{b}\ (\mathbf{a}\cdot\mathbf{c}) - \mathbf{c}\ (\mathbf{a}\cdot\mathbf{b})$, we finally arrive at the linearized expression for the scattering shift vector

$$\mathbf{R}_{s;\beta\beta}(\mathbf{k},\mathbf{k}') \approx (\mathbf{k}-\mathbf{k}')\times\mathbf{\Omega}_\beta(\mathbf{k}_0)\ , \tag{B.11}$$

where the vector $\mathbf{\Omega}_\beta(\mathbf{k}_0)$ is defined as

$$\mathbf{\Omega}_\beta(\mathbf{k}_0) = \nabla_k\times\xi_{\beta\beta}(\mathbf{k}_0) = i\sum_{\alpha\neq\beta}\ \mathbf{r}_{\beta\alpha}(\mathbf{k}_0)\times\mathbf{r}_{\alpha\beta}(\mathbf{k}_0)\ . \tag{B.12}$$

The last expression for $\nabla_k\times\xi_{\beta\beta}(\mathbf{k}_0)$ is also derived in Ref.[30] (Eqn.13). A standard analysis using the symmetry properties [14, 17] of the $\mathbf{r}_{\alpha\beta}(\mathbf{k}_0)$ shows that $\mathbf{\Omega}_\beta(\mathbf{k}_0)$ represents an axial pseudo-vector [10] and, as a consequence, can be nonzero only if the material does not posses a center of inversion. It can be evaluated numerically from *ab-initio* values of the respective matrix elements.

References

[1] B. I. Sturman and V. M. Fridkin, *The Photovoltaic and Photorefractive Effects in Non-centrosymmetric Materials*, Ferroelectricity and Related Phenomena V. 8, edited by G. W. Taylor (Gordon and Breach Science Publishers, (1992)); and references therein.

[2] G. Kurizki, M. Shapiro and P. Brumer, Phys. Rev. B **39**, 3435 (1989).

[3] E. Dupont *et al.*, Phys. Rev. Lett. **74**, 3596 (1995); R. Atanasov *et al.*, Phys. Rev. Lett. **76**, 1703 (1996).

[4] P. Král and J. Sipe, Phys. Rev. B. **61**, 5381 (2000).

[5] P. Král and D. Tománek, Phys. Rev. Lett. **82**, 5373 (1999); E. J. Mele, P. Král and D. Tománek, Phys. Rev. B **61**, 7669 (2000).

[6] J. M. Luttinger, Phys. Rev. **112**, 739 (1958).

[7] W. Kraut and R. v. Baltz, Phys. Rev. B **19**, 1548 (1979); *ibid* **23**, 5590 (1981).

[8] N. Kristoffel and A. Gulbis, Z Phys. B **39**, 143 (1980).

[9] V. I. Belinicher, E. L. Ivchenko, and B. I. Sturman, Sov. Phys. JETP **56**, 359 (1983).

[10] K. Busch, Diploma thesis, (University of Karlsruhe, 1992).

[11] V. I. Belinicher and B. I. Sturman, Ferroelectrics **83**, 29 (1988).

[12] R. Ya. Rasulov et al., Semiconductors **33**, 45 (1999); *references therein.*

[13] P. Král and J. E. Sipe, in *Progress in Nonequilibrium Green's functions*, edited by M. Bonitz, (World Scientific, Singapore 2000).

[14] E. I. Blount, in *Solid State Physics, Advances in Research and Applications*, edited by F. Seitz and D. Turnbull (Academic, New York, 1962), Vol. 13, p. 305.

[15] J. E. Sipe and Ed Ghahramani, Phys. Rev. B **48**, 11705 (1993).

[16] J. E. Sipe and A. Shkrebtii, Phys. Rev. B. **61**, 5337 (2000).

[17] O. Madelung, *Introduction to Solid State Theory*, (Springer-Verlag, New York 1978).

[18] G. D. Mahan, *Many-particle physics*, (Plenum, New York 1981).

[19] L. P. Kadanoff and G. Baym, *Quantum Statistical Mechanics*, (Benjamin, New York 1962).

[20] H. Haug and A.-P. Jauho, *Quantum Kinetics in Transport and Optics of Semiconductors*, Springer Series V.123, (New York 1996).

[21] Y. L.-Geller and J.-P. Leburton, Semic. Sci. and Technol. **10**, 1463 (1995).

[22] V. B. Sulimov, Sov. Phys. JETP **74**, 931 (1992).

[23] B. Spivak, F. Zhou and M. T. Beal Monod, Phys. Rev. B **51**, 13226 (1995).

[24] D. C. Langreth, in *Linear and Nonlinear Electron Transport in Solids*, edited by J. T. Devresee and E. van Boren (Plenum, New York, 1976).

[25] P. Král, Jour. of Stat. Phys. **86**, 1337 (1997).

[26] B. Adolph *et al.*, Phys. Rev. B **53**, 9797 (1996).

[27] R. Binder *et al.*, Phys. Rev. B **55**, 5110, (1997).

[28] P. Král, E. J. Mele, and D. Tománek, Phys. Rev. Lett., **85**, 1512 (2000).

[29] G. L. Bir and G. E. Pikus, *Symmetry and Strain-Induced Effects in Semiconductors*, (Wiley, New York, 1974).

[30] C. Aversa and J.E. Sipe, Phys. Rev. B **52**, 14636 (1995).